## PROCEEDINGS OF SPIE

SPIEDigitalLibrary.org/conference-proceedings-of-spie

# Metasurface-enhanced infrared spectroscopy for continuously monitoring the effect of cholesterol depletion in live cells

Huang, Steven, Delgado, Robert, Shvets, Gennady

Steven H. Huang, Robert Delgado, Gennady B. Shvets, "Metasurface-enhanced infrared spectroscopy for continuously monitoring the effect of cholesterol depletion in live cells," Proc. SPIE 11236, Biomedical Vibrational Spectroscopy 2020: Advances in Research and Industry, 112360P (21 February 2020); doi: 10.1117/12.2547141



Event: SPIE BiOS, 2020, San Francisco, California, United States

## Metasurface-enhanced infrared spectroscopy for continuously monitoring the effect of cholesterol depletion in live cells

Steven H. Huang, Robert Delgado, and Gennady Shvets\*
School of Applied and Engineering Physics, Cornell University, Ithaca, New York, USA 14853;
\*Email: gs656@cornell.edu

#### **ABSTRACT**

Surface-enhanced infrared absorption (SEIRA) based on top-down fabricated nanostructures such as nanoantennas and metasurfaces has attracted much attention in recent years. These plasmonic resonant nanostructures can enhance the IR absorption signal of nearby molecules through its nearfield enhancement and have been shown to be able to detect adsorbed monolayers of proteins and lipids through their IR absorption spectra. Here, we demonstrate the continuous monitoring of cellular responses to stimuli using metasurface-enhanced infrared spectroscopy (MEIRS). A431 cells are seeded on a gold plasmonic metasurface fabricated on CaF<sub>2</sub> substrate. Continuous monitoring is made possible by integrating the metasurface with a flow chamber, and the IR absorption spectra of the attached cells are measured in reflectance mode under continuous perfusion of cell culture medium. Scanning electron microscopy (SEM) revealed that the cells preferentially adhere to gold surfaces rather than CaF<sub>2</sub> surfaces, suggesting that the IR signal measured through MEIRS is highly sensitive to the cells' attachment and interaction with the gold metasurface. We have monitored the effect of methyl-beta-cyclodextrin, a cholesterol-depleting compound, on A431 cells. Principal component analysis highlighted the complex and subtle spectral changes of the cells.

**Keywords:** MIR spectroscopy, surface-enhanced infrared absorption, metasurface, metasurface enhanced infrared absorption, MEIRS, cell adhesion, methyl-beta-cyclodextrin, cholesterol

#### 1. INTRODUCTION

Infrared (IR) spectroscopy is a label-free and non-invasive technique that probes molecular fingerprint based on molecular vibrational bonds. In recent years, IR spectroscopy has received increasing interest for application in analyzing biological samples such as histological tissue sections, blood serum, and live tissues.<sup>1-4</sup> The molecular fingerprint of a biological sample observed through IR spectroscopy includes those of proteins, lipids, nucleic acids, and carbohydrates.<sup>1</sup> Due to the spectral data being often large and complex, multivariate statistical analysis and machine learning methods are usually used to analyze the data. With machine learning, drugs can be classified according to their mode of action on cells and a tissue section can be classified based on the type of tissue (for example, cancer vs. normal), all based on their IR spectral features.<sup>2,5</sup>

The IR absorption signal, however, is typically weak, requiring long integration time and a large number of averaging. This weak IR absorption can be enhanced in a process called Surface-Enhanced Infrared Absorption (SEIRA). SEIRA, much like the well-known Surface-Enhanced Raman Scattering (SERS), relies on analyte interaction with plasmonic nanostructures. When the analyte is within the hot spots created by these plasmonic nanostructures, the IR absorption can be enhanced by several orders of magnitude. SEIRA nanostructures can be larger than SERS nanostructures, allowing for a large array of geometries to be created through electron-beam lithography, including linear nanoantennas, nanoslits, and more complex geometries such as Fano-asymmetric metasurfaces and bowtie antennas. The sensitivity of these SEIRA nanostructures has already been demonstrated for measuring the IR spectra of self-assembled monolayers, proteins, lipid bilayers, as well as fixed and dried cells. 19,11

In this work, we further extend the application of SEIRA to the investigation of live cells using plasmonic gold metasurface, a technique we named metasurface-enhanced IR reflection spectroscopy (MEIRS). The cells are seeded on the metasurface, which is integrated with a flow chamber. During the measurement, the cells are maintained with continuous perfusion of culture media, and different compounds can be added to stimulate the cell, with the cell's response monitored through IR

Biomedical Vibrational Spectroscopy 2020: Advances in Research and Industry, edited by Wolfgang Petrich, Zhiwei Huang, Proc. of SPIE Vol. 11236, 112360P ⋅ © 2020 SPIE CCC code: 1605-7422/20/\$21 ⋅ doi: 10.1117/12.2547141

spectroscopy continuously in real-time. Whereas previous optical techniques for phenotypical cell monitoring, such as surface plasmon resonance and optical grating-based systems, <sup>12,13</sup> only track the change in one value (for example, resonance frequency), MEIRS collects an entire spectrum consisting of hundreds of wavenumber points, potentially increasing the amount of information we can extract out from the measurement.

As a proof of concept experiment, we tested the response of A431 cells to cholesterol depletion using methyl-beta-cyclodextrin (MBCD). In mammalian cells, cholesterol is a major component of the cell membrane and is essential to various processes such as cell signaling, membrane fluidity, and lipid sorting. MBCD leads to acute depletion of cholesterol from cellular membranes by binding to cholesterol and forming a water-soluble complex, thus extracting cholesterol from cellular membranes. HBCD is the most common method for cholesterol depletion from live cells and its effect on cells have been characterized by other optical phenotypic assays previously. HBCD with cholesterol, one can form MBCD-cholesterol complex (MBCD-chol), which may enrich membrane cholesterol instead of depleting it and can be used as a control to determine if an observed change is indeed related to cholesterol depletion.

#### 2. EXPERIMENTAL PROCEDURE

Fano-resonant asymmetric metasurfaces were fabricated as previously described. <sup>10,11</sup> Briefly, polymethyl methacrylate (PMMA) e-beam resist was spin-coated on a 12.5 mm x 12 mm x 0.5 mm CaF<sub>2</sub> substrate and metasurface patterns were defined through electron beam lithography. 5 nm of Cr adhesion layer followed by 70 nm of Au layer was evaporated on to the resulting structure and the metasurface pattern was transferred to the Au layer through lift-off in an acetone bath. A scanning electron microscopy (SEM) image of the metasurface is shown in Figure 1 (a) and (b).

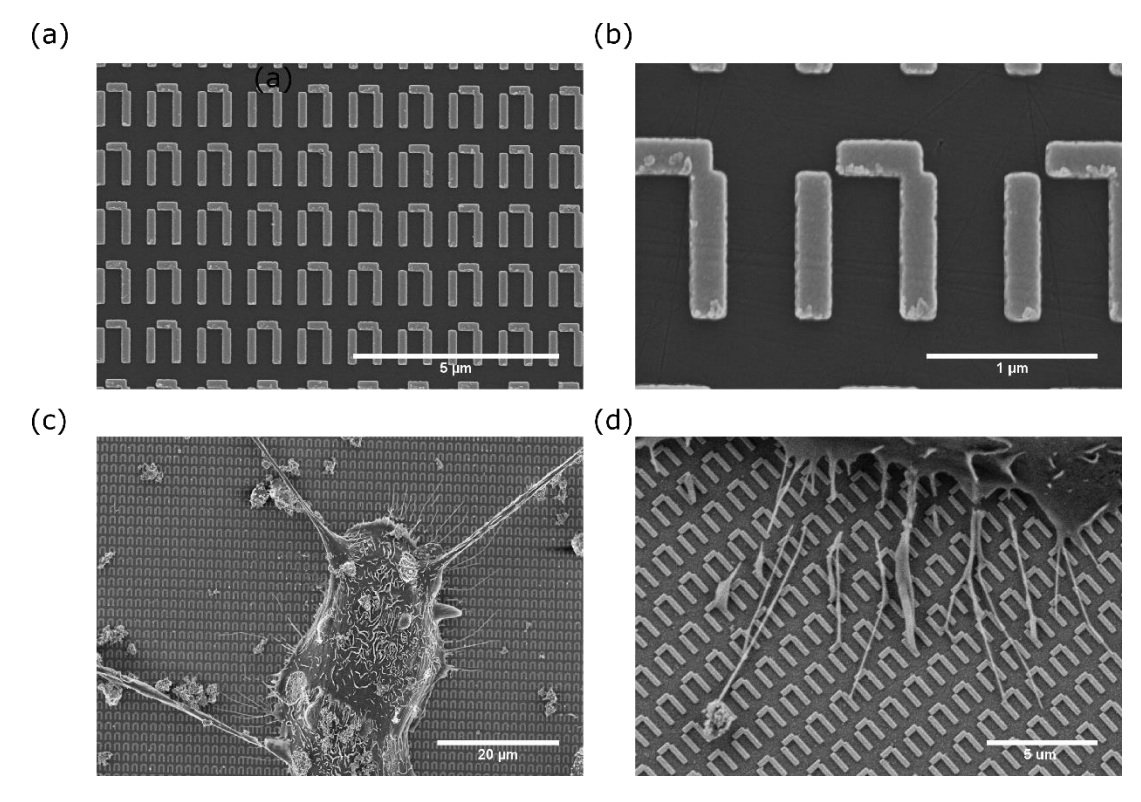


**Figure 1**. SEM images of the metasurface ((a) and (b)), as well as A431 cells grown on metasurface ((c) and (d)). Filopodia of the cell are seen mostly attached to the gold nanoantennas rather than the CaF<sub>2</sub> substrate in (d).

Before seeding the cells, the metasurface was incubated overnight in  $10~\mu g/mL$  fibronectin solution in Dulbecco's phosphate-buffered saline (DPBS) and washed with DPBS twice. Human epidermoid carcinoma cell line A431 cells were obtained from the American Type Culture Collection (ATCC) and cultured in Dulbecco's Modified Eagle Medium (DMEM) supplemented with 10~% fetal bovine serum (FBS) and 1~% penicillin-streptomycin. A431 cells were detached from culture flask using 0.25% trypsin-EDTA and seeded on the fibronectin-coated metasurface in a 12~well dish. The cells were incubated on the metasurface in DMEM + 10% FBS until confluent coverage (>95%) was achieved. Before measurement, the cells were serum-starved overnight in DMEM with no serum.

For measurement with IR spectroscopy, The metasurface with cells was taken out from the 12 well plate and assembled on a polydimethylsiloxane (PDMS) flow chamber, as showing in Figure 2. The flow chamber is connected to a syringe pump to constantly perfuse the chamber with fresh media at a flow rate of 0.1  $\mu$ L/s. Leibovitz's L-15 medium was used during spectroscopic measurement to maintain pH in ambient conditions. A microscope stage heater is placed under the flow chamber to maintain the temperature at 37 °C.

IR spectra were collected in reflection mode using Bruker Hyperion 3000 IR microscope with a 15X Cassegrain objective and a single element HgCdTe (MCT) detector, coupled with Bruker Vertex 70 Fourier Transform IR spectrometer. Unpolarized light was used for the measurement. Spectra were collected at 4 cm<sup>-1</sup> resolution, 120 averaging, and one acquisition per minute.

The flow chamber setup was mounted on the IR microscope and media flow was kept for at least one hour before MBCD was introduced to obtain a stable baseline. 10 mM MBCD or MBCD-chol in L-15 was injected into the flow chamber at  $0.1 \,\mu\text{L/s}$ , and the reflectance spectrum from the metasurface was continuously monitored for 5-10 hours. MBCD-chol was prepared as previously described. <sup>13</sup> Briefly, 10 mM MBCD in L15 was mixed with excess cholesterol and agitated overnight at 37 °C. The excess cholesterol crystals were filtered out from the resulting solution before use.

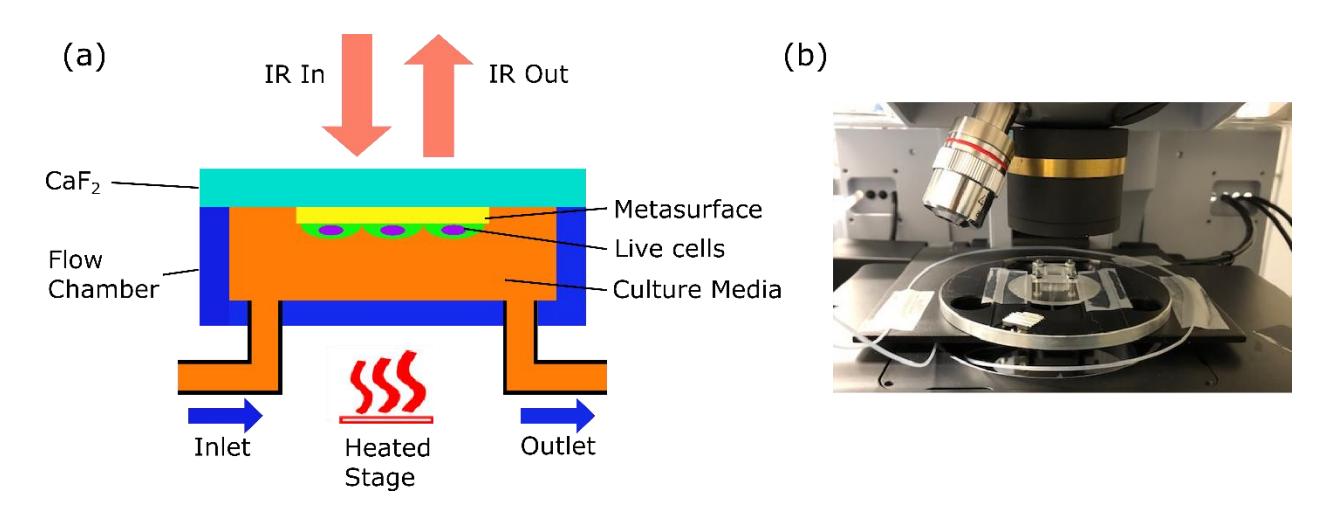


**Figure 2**. Measurement setup. (a): Schematic drawing of the flow chamber. (b): Photograph of the actual flow chamber, mounted on a microscope heater under a reflective Cassegrain objective.

### 3. RESULT

A431 cells grown on the metasurface were fixed and dried for SEM imaging, as shown in Figure 1 (c) and (d). As seen from Figure 1 (d), the filopodia extending out from the cell periphery mostly attach to the gold nanoantenna rather than the CaF<sub>2</sub> substrate. Such attachment pattern suggests that the cells preferentially form adhesion sites on gold structures rather than CaF<sub>2</sub>. Simulation results indicate that the optical nearfield is localized in the vicinity of these plasmonic nanoantennas (data not shown). Although the SEIRA enhancement factor from metasurface is difficult to predict due to

the highly irregular shapes of the cells, such close contact between the cells and the gold nanoantennas suggests high signal enhancement at these attachment sites.

The reflectance spectra of the metasurface with and without cells are presented in Figure 3. The Fano-resonant asymmetric metasurfaces support two resonances, a dipolar mode and a quadrupolar mode, with the quadrupolar mode appearing as a Fano resonance at close to 2000 cm<sup>-1</sup>. The spectral position of these modes can be tuned by changing the geometrical parameters of the nanoantennas and these parameters were adjusted to match the resonance position to molecular vibrations of interest. IR absorption bands from cells appear as small perturbations on top of the reflectance spectrum of the metasurface. Comparing between the metasurface reflectance spectra with and without cells, we see large overlap between the two, but with significant differences in the spectral regions of 1500 – 1700 cm<sup>-1</sup> (Figure 3 (b)), 1900 – 2200 cm<sup>-1</sup> (Figure 3 (c)), and 2850 – 3050 cm<sup>-1</sup> (Figure 3 (d)). These differences are attributed to absorption from amide I (1550 cm<sup>-1</sup>) and amide II (1660 cm<sup>-1</sup>) vibrational bands from proteins, shift in the Fano resonance due to refractive index change, and absorption from CH<sub>2</sub> and CH<sub>3</sub> vibrations from lipids. Note that the large dip in metasurface reflectance at 1660 cm<sup>-1</sup> is due to the IR absorption from liquid water.

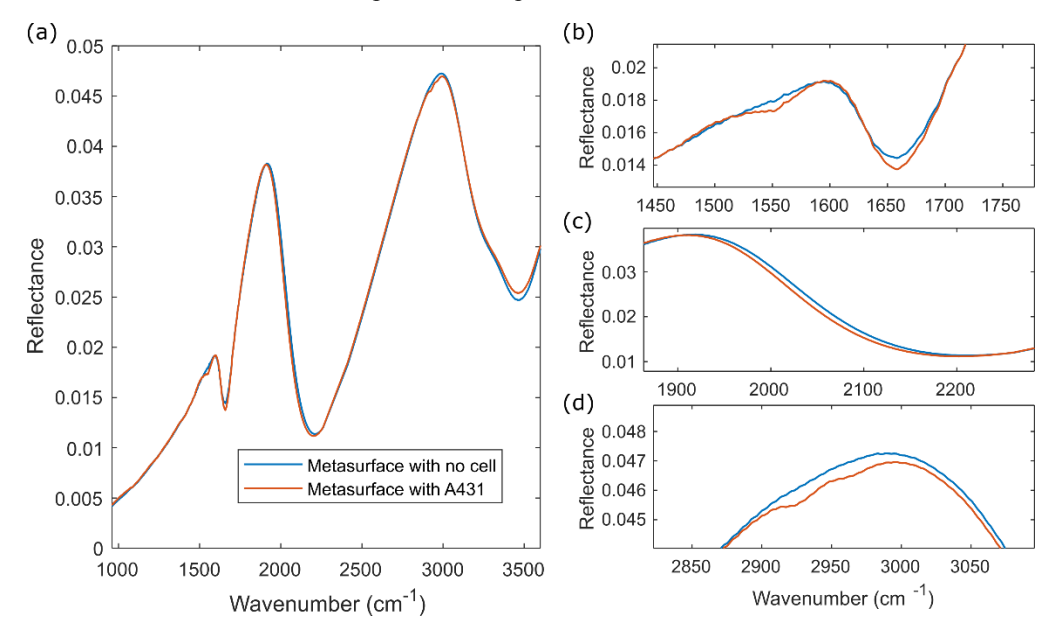


**Figure 3**. Reflection spectra of the metasurface with and without cells. (b)-(d) shows the same reflectance spectra, zoomed in to protein absorption (b), Fano resonance shift (c), and lipid absorption (d).

The spectral response of A431 cells to MBCD is presented in Figure 4. Figure 4 (a) shows the change in the measured absorbance, calculated as  $A = -\log_{10}(R/R_0)$ , where  $R_0$  is the reflectance spectrum at t = 0. MBCD solution arrives at the flow chamber at approximately t = 45 min. The spectral response shows a complex behavior with different temporal responses for different wavenumbers. To reduce the complexity, principal component analysis (PCA) was used for dimensionality reduction. It was found that the first two principal components explained more than 99% of the variance. These two components were further rotated by Promax rotation and the resulting component loadings and scores are shown in Figure 4 (b) and (c). The loadings show the spectral content of each component, while the scores show their temporal response.

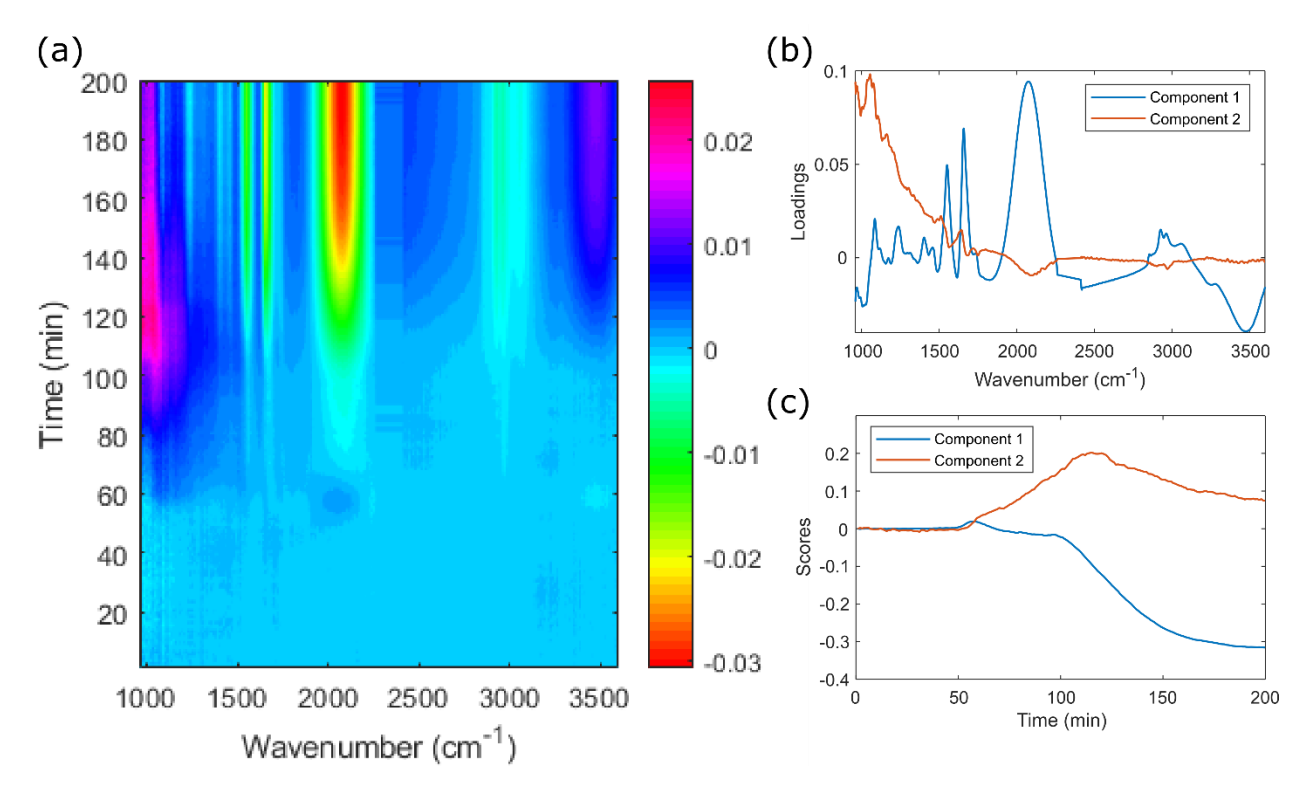


**Figure 4.** Spectral changes of A431 cells in response to 10 mM MBCD. (a): Color plot of the change in absorbance spectra. (b): Component loadings from PCA followed by Promax rotation (c): Component scores from PCA followed by Promax rotation.

In component 1 loading, we can identify the typical IR absorbance peaks attributed to biological matters, including amide I ( $1660 \text{ cm}^{-1}$ ) and amide II ( $1550 \text{ cm}^{-1}$ ) peaks from proteins,  $CH_2$  and  $CH_3$  vibrations attributed to lipids ( $2800 - 3000 \text{ cm}^{-1}$ ), phosphate peaks at  $1090 \text{ cm}^{-1}$  and  $1240 \text{ cm}^{-1}$ , as well as several smaller absorption peaks. The largest peak at  $2080 \text{ cm}^{-1}$  is attributed to the shift in Fano resonance due to refractive index change. The temporal response curve of component 1 is relatively flat until t = 100 min when it begins to change abruptly until the response saturates at t = 200 min. This is attributed to the detachment of the cells from the metasurface. We confirmed this behavior in a parallel experiment observed under visible microscopy, in which upon introduction of MBCD, the cells began to shrink and decrease in coverage on the metasurface, until they were eventually completely detached from the metasurface.

In contrast to component 1, component 2 loading shows little features that can be attributed to absorption peaks. Instead, the predominant feature is a sloping baseline extending from  $1000 \text{ cm}^{-1}$  to  $2000 \text{ cm}^{-1}$ . It is not clear what leads to this spectral change, but it may be connected to changes in cell morphology in response to MBCD. Component 2 starts to change as soon as MBCD is introduced and changes in slope at around t = 115 min. This slope change may be connected to cell detachment, as evident from component 1.

Focusing on the Fano resonance shift around 2080 cm<sup>-1</sup>, we also see some distinct changes from t = 50 min to t = 70 min, not seen in other absorption bands. Due to the small magnitude of this change, it is difficult to separate it using PCA. Instead, we integrate the Fano shift peak to focus on the refractive index change, excluding the contribution from other absorption bands and baseline changes (Figure 5). The response from 10 mM MBCD is compared with that of 10 mM MBCD-chol. As shown in Figure 5, the cell's spectral response to MBCD can be divided into three phases. Phase 1 response scales with the concentration of MBCD and the response is present even if there is no cell (data not shown), and thus it is attributed to the increase in refractive index due to having MBCD dissolved in the media. Phase 2 response is seen in the cholesterol depleting MBCD treatment but no change is seen in the MBCD-chol treatment, which does not

deplete cholesterol. This change may be directly related to cholesterol extraction from the cell membrane, as seen from a previous study using surface plasmon resonance to monitor cholesterol depletion.<sup>13</sup> This cholesterol depletion in MBCD treated cells further leads to cell detachment from metasurface in phase 3, possibly by triggering one of the cellular signaling pathways.<sup>12</sup>

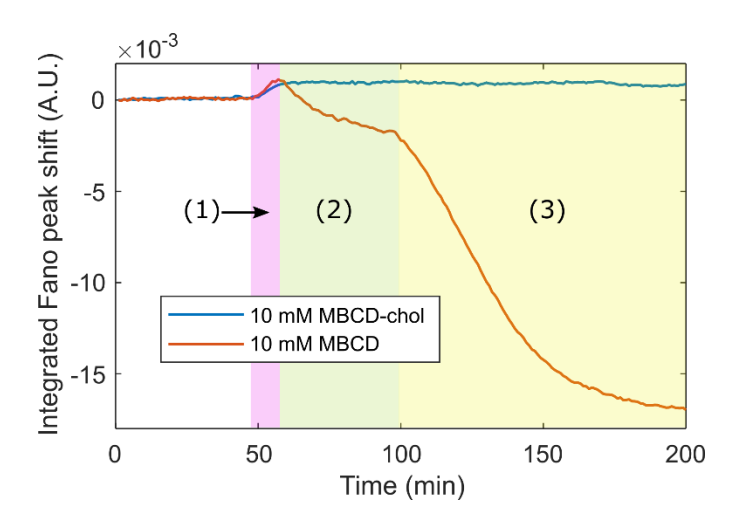


Figure 5. Cell's response to MBCD and MBCD-chol, as visualized by the shift in Fano resonance.

#### 4. CONCLUSION

In conclusion, we have monitored A431 cells using MEIRS in real-time and observed the cell's spectral changes in response to treatment by MBCD. A431 cells showed preferential attachment to gold nanoantennas, suggesting that IR absorption enhancement using plasmonic hotspots from gold nanostructures could be an effective way to enhance the IR absorption signal. We observed that the cells showed a complex spectral change that could be divided into several different phases, with the strongest signal coming from their detachment from metasurface. Although we still have remaining questions regarding how to explain the observed spectral change, it is clear that real-time monitoring of IR spectra can resolve different components, corresponding to different processes occurring in the cell simultaneously. We envision that MEIRS would have an important application in many areas such as drug screening and cancer research.

#### ACKNOWLEDGEMENT

This work was performed in part at the Cornell NanoScale Facility, a member of the National Nanotechnology Coordinated Infrastructure (NNCI), which is supported by the National Science Foundation (Grant NNCI-1542081). This work made use of the Cornell Center for Materials Research Shared Facilities which are supported through the NSF MRSEC program (DMR-1719875).

#### REFERENCES

- 1. Baker, M. J. *et al.* Using Fourier transform IR spectroscopy to analyze biological materials. *Nat. Protoc.* **9**, 1771–1791 (2014).
- 2. Mittal, S. *et al.* Simultaneous cancer and tumor microenvironment subtyping using confocal infrared microscopy for all-digital molecular histopathology. *Proc. Natl. Acad. Sci.* **115**, E5651–E5660 (2018).
- 3. Butler, H. J. *et al.* Development of high-throughput ATR-FTIR technology for rapid triage of brain cancer. *Nat. Commun.* **10**, 1–9 (2019).
- 4. Andrew Chan, K. L. & Kazarian, S. G. Attenuated total reflection Fourier-transform infrared (ATR-FTIR) imaging of tissues and live cells. *Chem. Soc. Rev.* **45**, 1850–1864 (2016).
- 5. Mignolet, A., Derenne, A., Smolina, M., Wood, B. R. & Goormaghtigh, E. FTIR spectral signature of anticancer drugs. Can drug mode of action be identified? *Biochim. Biophys. Acta Proteins Proteomics* **1864**, 85–101 (2016).
- 6. Neubrech, F., Huck, C., Weber, K., Pucci, A. & Giessen, H. Surface-enhanced infrared spectroscopy using resonant nanoantennas. *Chem. Rev.* **117**, 5110–5145 (2017).
- 7. Rodrigo, D. *et al.* Resolving molecule-specific information in dynamic lipid membrane processes with multi-resonant infrared metasurfaces. *Nat. Commun.* **9**, 2160 (2018).
- 8. Huck, C. *et al.* Plasmonic Enhancement of Infrared Vibrational Signals: Nanoslits versus Nanorods. *ACS Photonics* **2**, 1489–1497 (2015).
- 9. Dong, L. *et al.* Nanogapped Au Antennas for Ultrasensitive Surface-Enhanced Infrared Absorption Spectroscopy. *Nano Lett.* **17**, 5768–5774 (2017).
- 10. Wu, C. *et al.* Fano-resonant asymmetric metamaterials for ultrasensitive spectroscopy and identification of molecular monolayers. *Nat. Mater.* **11**, 69–75 (2011).
- 11. Kelp, G. *et al.* Application of metasurface-enhanced infra-red spectroscopy to distinguish between normal and cancerous cell types. *Analyst* 1115–1127 (2019).
- 12. Fang, Y., Ferrie, A. M. & Li, G. Cellular functions of cholesterol probed with optical biosensors. *Biochim. Biophys. Acta Mol. Cell Res.* **1763**, 254–261 (2006).
- 13. Ziblat, R., Lirtsman, V., Davidov, D. & Aroeti, B. Infrared surface plasmon resonance: A novel tool for real time sensing of variations in living cells. *Biophys. J.* **90**, 2592–2599 (2006).
- 14. Owen, D. M. Methods in Membrane Lipids. Humana Press 1232, (2015).